

Derivation of buckling design curves via FE modelling for in-plane compressed timber log-walls in accordance with the Eurocode 5

Chiara Bedon^{1*}, Massimo Fragiaco²

Abstract

In ‘*Blockhaus*’ systems the structural capacity derives from surface interactions and friction mechanisms between multiple timber logs stacked horizontally one upon each other. Unlike masonry or concrete walls, timber log-walls are characterized by the absence of a full structural interaction between the basic components, hence resulting in ‘assembled’ rather than ‘fully monolithic’ structural systems characterized by high flexibility of timber and usually high slenderness ratios. The current Eurocode 5 for timber structures, however, does not provide formulations for the prediction of the critical load of log-haus walls under in-plane compressive loads.

In this work, based on past experimental tests and detailed Finite-Element (FE) models, extended numerical investigations are performed on timber log-walls. A wide number of configurations (more than 900) characterized by different geometrical properties, timber log cross-sections, number and position of door and window openings, presence of in-plane rigid (RF) or fully flexible (FF) inter-storey floors, as well as initial curvatures and/or load eccentricities, are analyzed under monotonic in-plane compressive load. Careful consideration is also given to the influence of additional out-of-plane pressures (e.g. wind pressures) combined with the in-plane compressive load. In accordance with the buckling design approach proposed by the Eurocode 5 for timber columns, non-dimensional buckling curves are then proposed for timber log-walls under in-plane compression. These curves are based on an accurate calibration of the k_c buckling coefficient and the related imperfection factors on the results of the numerical parametric study. The developed simple and conservative approach for the design of log-walls can be proposed for implementation in the new generation of the Eurocode 5.

Keywords: buckling, design method, FE model, timber log-walls

¹ University of Trieste, Department of Engineering and Architecture, Piazzale Europa 1, 34127 Trieste, Italy.
(*): corresponding author. Email: bedon@dicar.units.it; phone: +39 040 558 3837; fax: +39 040 558 3580.

² University of L’Aquila, Department of Civil, Construction-Architectural & Environmental Engineering, Via Giovanni Gronchi 18 - Zona industriale di Pile, 67100 L’Aquila, Italy

1. Introduction

Blockhaus structural systems are commonly obtained by assembling multiple timber logs, which are stacked horizontally on the top of one another. Although based on conceptually simple resisting mechanisms, the structural behaviour of *Blockhaus* systems is rather complex to predict. For this reason, hardly any design recommendations are available in current timber standards. Since metal connectors are generally avoided or minimized, the typical *Blockhaus* wall can sustain the vertical loads as far as a minimum level of contact among the logs is ensured. At the same time, the very low modulus of elasticity (MOE) of timber in the direction perpendicular to the grain makes the usually slender *Blockhaus* walls rather susceptible to flexural buckling, hence requiring the implementation of analytical design models. Compared to structural members and assemblies made of steel, for example, the buckling resistance of timber structural systems markedly depends upon the mechanical constitutive behaviour and intrinsic anisotropy of the basic material. As a result, standardized and simplified analytical models available in current standards for steel and masonry structures (e.g. EN 1993-1-1: 2005, EN 1996-1-1: 2005) cannot be directly extended to timber log-walls and structural assemblies in general (Leicester 2009). Over the past decades, several authors studied the buckling response of single wooden members or timber assemblies, in order to provide useful design recommendations, practical rules, as well as to assess the potential of using additional reinforcements. The lateral-torsional buckling behaviour of timber beams has been investigated in (Baláz (2005)) and (Xiao et al. (2014)). Rodman et al. (2013) and Zahn (1973) focused respectively on the lateral stability of timber arches and wood beam-and-deck systems, while Eilering and Beißner (2011) assessed the buckling resistance of curved, circular glue-laminated beams. Hofmann and Kuhlmann (2014) proposed a simplified torsional buckling design method for glue-laminated timber girders. Regarding the structural stability of timber members and assemblies subjected to mainly compressive loads, analytical, experimental and Finite-Element studies related to buckling can be found in (Malhotra 1989; Theiler et al. 2013; Kessel 2012; Haller et al. 2014). The structural effects of additional reinforcements (e.g. fiber-reinforced plastic sheets, or fiber materials and screws) on the compressive buckling behaviour of timber columns have been assessed in (Taheri et al. 2009; Namiki and Nasu 2014). Schnabl et al. (2011) studied the effects of fire on the buckling resistance and response of timber columns, while in Bouras et al. (2010, 2012) the compressive cyclic buckling response of timber columns under repeated loading has been investigated by means of experimental tests and FE models.

This paper presents the implementation and calibration of standardized Eurocode-based design curves for the buckling verification of timber log-walls. In doing so, the typical buckling behaviour of vertically compressed timber log-walls and the effects of various mechanical and geometrical variables such as possible load eccentricities and/or initial curvatures, openings (e.g. doors or windows), fully flexible or in-plane rigid inter-storey floors are first assessed and investigated by means of detailed Finite-Element (FE) numerical models. All the FE investigations are preliminary

validated against buckling test results available in literature both for small-scale prototypes and full-scale log-walls (Heimeshoff and Kneidl 1992a; Heimeshoff and Kneidl 1992b; Bedon et al. 2015). By taking into account a wide set of geometrical configurations of practical interest, the effects of the main input parameters on the observed compressive buckling responses of timber log-wall systems are first highlighted. In order to provide buckling design recommendations of practical use and general applicability to mainly compressed timber log-walls, normalized design curves derived from standards (e.g. the buckling design approach provided in the Eurocode 5 for timber members in compression) are then properly calibrated on the basis of the results derived from an extensive FE numerical parametric study.

2. *Blockhaus* structural systems and design concepts

In current practice (e.g. www.rubnerhaus.com), a traditional *Blockhaus* log-wall with height H and length L is obtained by stacking horizontally a series of logs, for example made of spruce with strength class C24 according to (EN 338: 2009). These logs typically have cross-sectional dimensions of height h by width b , with the h/b ratio being between 1.6 and 2.4, and are characterized by small protrusions and tongues that are able to provide interlocking with the upper and lower logs (Fig.1a). Several log-wall profiles characterized by specific geometrical properties and by the possible use of different wood types (e.g. Fig.1d) are available on the market (see for example Figs.1b-1e). In some cases, the h/b ratio of the logs can decrease up to ≈ 0.8 . Fully rounded logs (Fig.1e) can also be used. Independently of the cross-sectional properties of logs, however, the design concept and structural assembly of log-wall structural systems is strictly related to interlocking of multiple timber elements. In *Blockhaus* buildings, the structural interaction between the main perpendicular walls composing the full structural assembly is in fact provided by appropriate corner joints (Figs.1f and 1g).

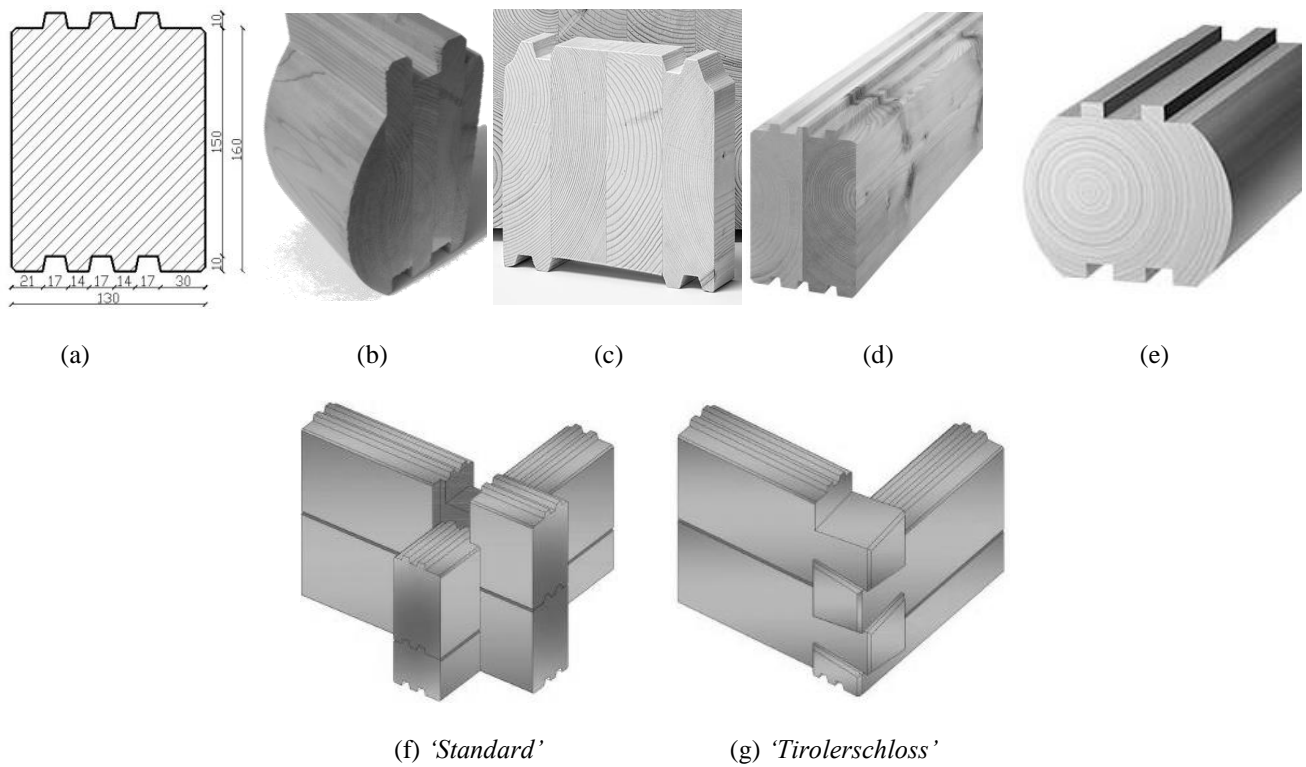


Fig. 1 Examples of 'Blockhaus' log cross-sections ((a) to (e)) and corner joints (f, g).

(a, f, g) www.rubnerhaus.com (dimensions in cm); (b): www.linclonlogs.com; (c): www.polarlifehaus.com;

(d): www.eurowood.co.nz; (e): www.satterwhite-log-homes.com

Each log-wall is connected to the RC foundation slab by means of steel angular brackets. The permanent gravity loads are thus transferred onto each main wall by the inter-storey floors. Depending on their assembly, these inter-storey floors can realize an in-plane rigid diaphragm (e.g. by using either OSB panels, timber joists and blocking, with the OSB sheathing properly nailed along the entire perimeter, or glulam panels arranged on their edges with proper connection between adjacent panels), hence resulting in a further lateral restraint able to avoid possible out-of-plane deflections of the wall top logs (Fig.2).

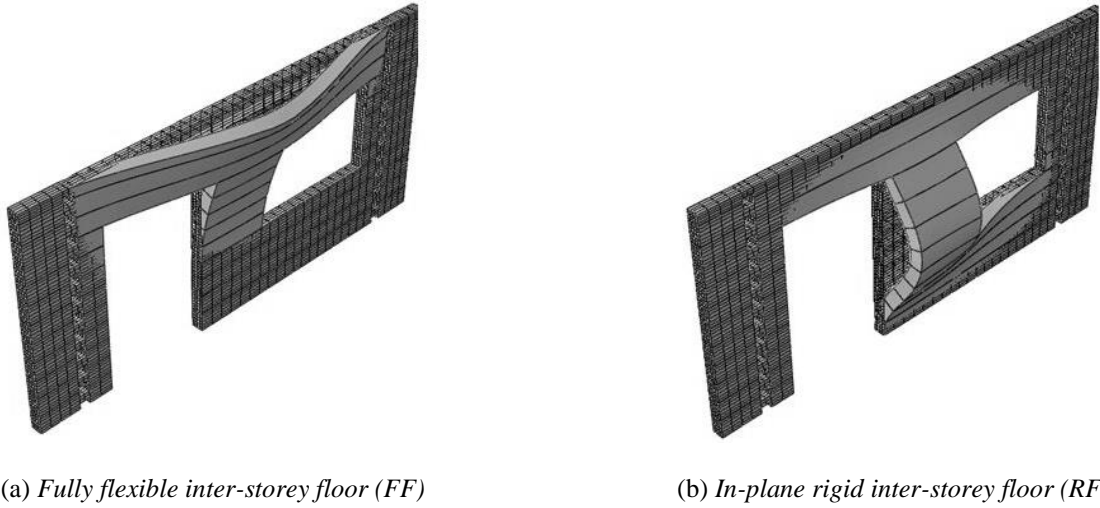


Fig. 2 Qualitative fundamental buckling shape for log-walls with (a) fully flexible or (b) in-plane rigid inter-storey floor, under in-plane compressive loads (Bedon and Fragiaco 2015)

3. Existing design methods for flexural buckling of timber structural members

3.1. Log-wall assemblies

The current Eurocode 5 for timber structures (EN 1995-1-1: 2005) does not provide formulations for the prediction of the critical load of log-walls under in-plane compressive loads.

In order to provide some practical design recommendations, an analytical and FE investigation was presented in (Bedon and Fragiaco 2015). In that paper, a preliminary assessment and calibration of closed-form formulations derived from classical buckling theories for the calculation of the compressive buckling resistance of timber log-walls was discussed. Validation of the implemented FE models was then carried out against full-scale buckling experiments discussed in (Bedon et al. 2015), as well as small-scale buckling experiments presented in (Heimeshoff and Kneidl 1992a) and (Bedon et al. 2015) for log-wall prototypes subjected to mid-span compressive loads. Based on the performed FE parametric studies, it was shown that the critical buckling load of a given log-wall with top rigid lateral restraint (RF) can be calculated as (see also Fig. 3):

$$N_{cr,0}^{(E)} = k_{\sigma} \frac{\pi^2 b^3}{12 L} \frac{E_{\perp}}{(1-\nu^2)} = k_{\sigma} \frac{\pi^2 b^3}{12 L} \frac{E_{\perp}}{\left(1 - \left(\frac{E_{\perp}}{2G} - 1\right)^2\right)} \quad (1)$$

with $k_{\sigma} = 6.97$ for log-walls without openings and $k_{\sigma} = 1.277$ for log-walls with a single door/window opening (with $L = L_{ef}$ the reference length in Eq.(1), in accordance with Fig. 3a). In Eq.(1), E_{\perp} and G denote respectively the MOE in the direction perpendicular to the grain and the average shear modulus of the timber.

If double door/window openings are present, the theoretical critical buckling load is given by:

$$N_{cr,0}^{(E)} = \frac{\pi^2 (EI_{ef})}{\bar{H}^2}, \quad (2)$$

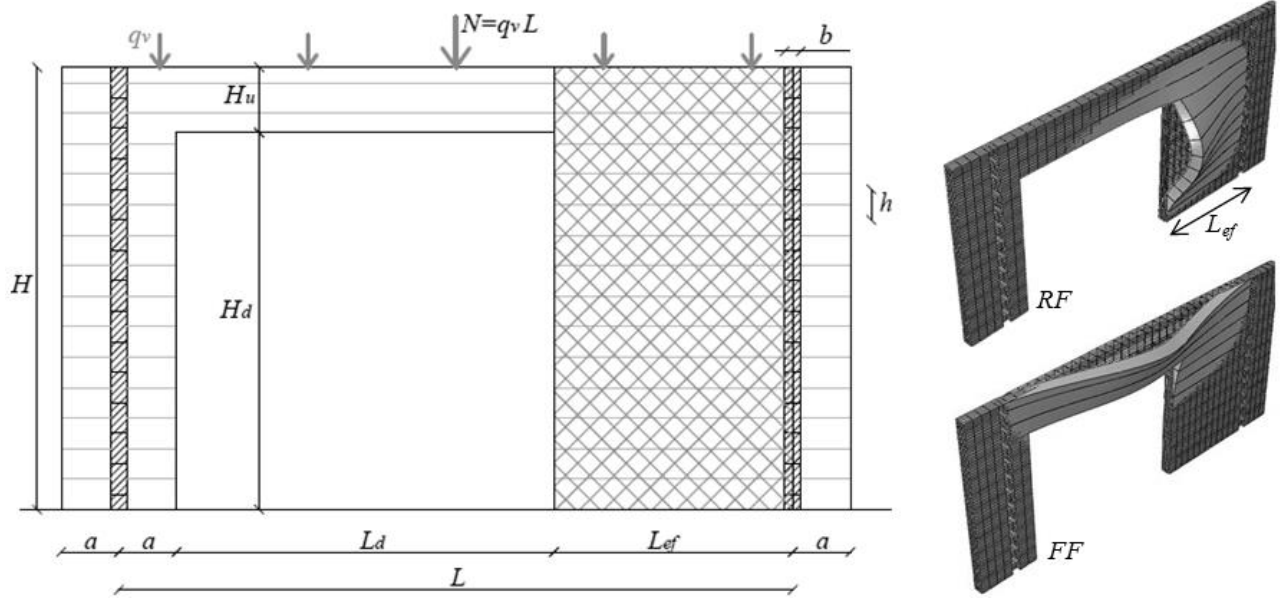
where (see Fig. 3):

$$\bar{H} = 0.7H_d \quad (3)$$

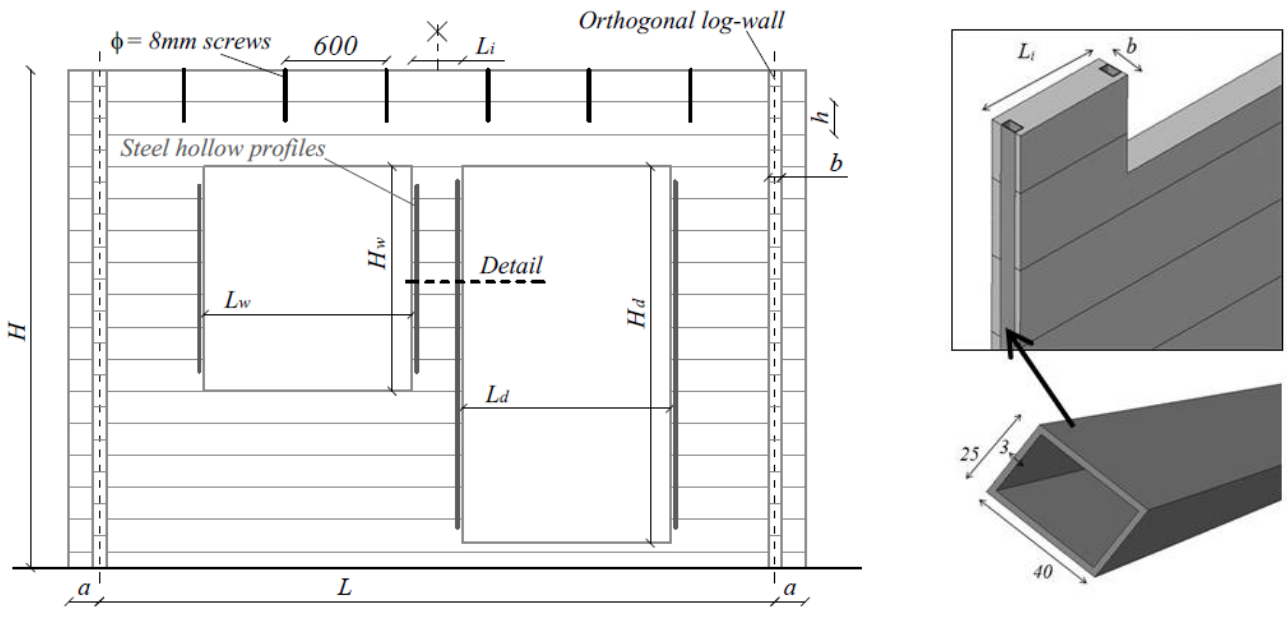
and

$$EI_{ef} = E_{\perp} \frac{b^3 L_i}{12} + 2E_{steel} I_{steel} \quad (4)$$

represents the equivalent bending stiffness of the 'composite' portion of wall with metal stiffeners (see Fig. 3b).



(a)



(b)

Fig. 3 (a) Example of a log-wall configuration with single door opening, with the corresponding buckling collapse mechanism; (b) log-wall with double door and window openings, and details of the metal steel hollow profiles introduced along their vertical edges (www.rubnerhaus.com) (dimensions in mm)

As shown in (Bedon and Fragiaco 2015) by means of extended comparative investigations, Eqs.(1) and (2) can predict with close accuracy the Euler's critical load of timber log-walls of various geometrical properties, leading – especially for single or double door/window openings – to conservative estimations of the expected theoretical resistance for the same log-walls. A further imperfection factor was also proposed in (Bedon and Fragiaco 2015), so that based on the expected value of the theoretical compressive buckling resistance $N_{cr,0}^{(E)}$ (e.g. Eqs.(1) or (2)), the actual load-carrying capacity of a given log-wall affected by possible initial geometrical curvatures and/or load and boundary eccentricities could be estimated as:

$$N_{cr} = \chi_{imp} N_{cr,0}^{(E)} \quad (5)$$

where

$$\chi_{imp} = \left(1 - \frac{e_{tot}}{b} \right) \quad (6)$$

and $e_{tot} \equiv (u_{0,max} + e_{load})$, with $u_{0,max} \geq H/400$ the minimum recommended curvature amplitude.

3.2. Timber members in compression

In accordance with the Eurocode 5 (EN 1995-1-1-2005, point 6.3. “*Stability of members*”), a standardized buckling design method for log-walls under in-plane compression could take the form of non-dimensional curves, properly calibrated so that the effects deriving from a multitude of mechanical and geometrical parameters (e.g. material mechanical properties, initial curvatures, load and boundary eccentricities, etc.) could be taken into account and result in conservative buckling predictions. Based on the Eurocode 5 approach, for example, the buckling verification of a timber column under compression is performed by taking into account its minimum relative slenderness ratio:

$$\lambda_{rel} = \frac{\lambda}{\pi} \sqrt{\frac{f_{c,0,k}}{E_{0.05}}}, \quad (5)$$

where

$$\lambda = \frac{L_0}{\rho_{min}} = L_0 \sqrt{\frac{A}{I_{min}}}, \quad \text{with } A \text{ the cross-sectional area,} \quad (6)$$

$f_{c,0,k}$ is the characteristic compressive strength parallel to the grain and

$E_{0.05}$ represents the fifth percentile value of the MOE parallel to the grain.

The stability check of the member in pure compression requires that the design compressive stress $\sigma_{c,0,d}$ along the member would satisfy the condition:

$$\sigma_{c,0,d} \leq k_c \cdot f_{c,0,d}, \quad (7)$$

where $f_{c,0,d}$ signifies the design compressive strength in the direction parallel to the grain and k_c denotes a buckling reduction factor given by:

$$k_c = \frac{1}{k + \sqrt{k^2 - \lambda_{rel}}}, \quad (8)$$

with

λ_{rel} defined by Eq.(5)

k a coefficient taking into account the effects of initial imperfections, given by:

$$k = 0.5 \cdot \left(1 + \beta_c (\lambda_{rel} - \beta_0) + \lambda_{rel}^2 \right), \quad (9)$$

β_c an imperfection factor equal to 0.2 or 0.1 for solid timber or glued laminated timber and LVL, respectively, while the coefficient $\beta_0 = 0.3$ in Eq.(9), finally, represents the minimum relative slenderness ratio λ_{rel} beyond which flexural buckling phenomena may occur in the column.

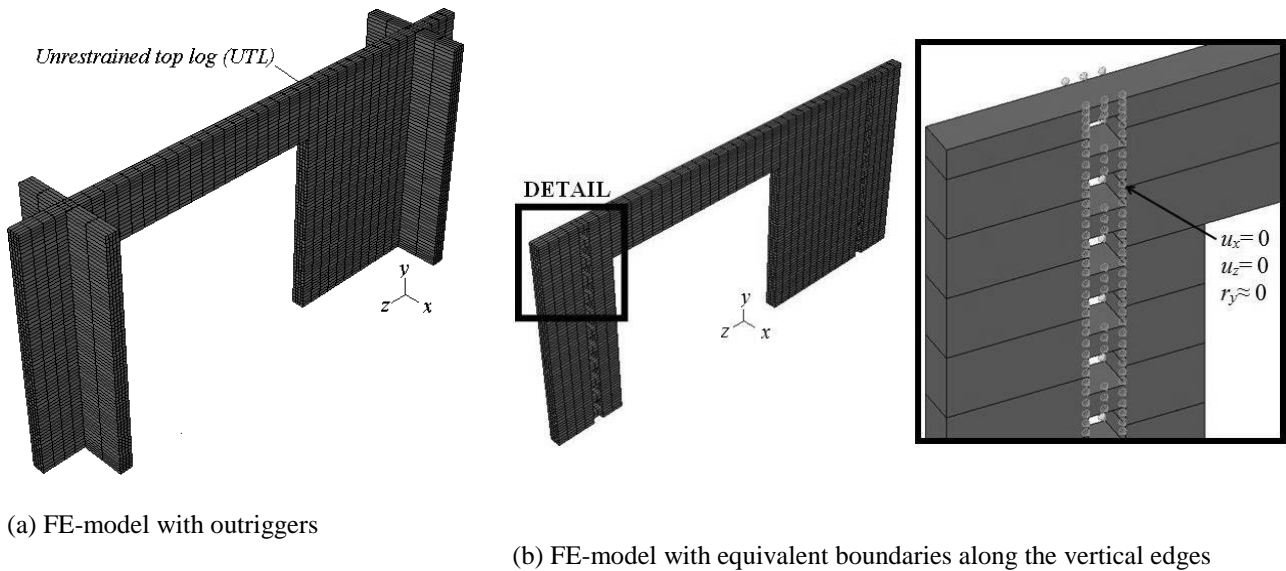
In accordance with the Eurocode 5 buckling design approach for timber columns, a standardized design method consisting of non-dimensional buckling curves is proposed in this work for timber log-walls under in-plane compression (Fig. 3).

The novelty of the current proposal is given by the accurate calibration and validation of normalized buckling design procedures and their application to the studied structural system. In doing so, the specific behaviour and resistance of in-plane compressed timber log-walls is described through imperfection factors, which were derived via FE numerical modelling. Such imperfection factors take into account the additional effects deriving from the log-walls discontinuity that increases the susceptibility to out-of-plane deformations and buckling phenomena with respect to the case of continuous timber columns. The final result of the current research project, in accordance with Eq.(7), is the proposal of a standardized design approach where the actual buckling resistance of a generic timber log-wall could be calculated – for each specific configuration – as a k_c fraction of the corresponding Euler's critical load.

4. Extended Finite-Element investigations

4.1. General numerical approach

The typical Finite-Element (FE) model used in this investigation consisted of 8-node, linear brick, solid elements with reduced integration (C3D8R), available in the ABAQUS element library (Simulia 2012). In each numerical simulation, a single log-wall laterally restrained by two portions of orthogonal log-walls working as outriggers is analysed (Fig. 4). Each timber log is described with a regular $b \times h$ cross section. While the characteristic small protrusions and tongues along the top and bottom surfaces of logs (Figs. 1a-1e) were reasonably neglected, the nominal geometry of logs near their end restraints, as well as near the doors or windows openings, was correctly reproduced (Fig. 4). In accordance with (Bedon and Fragiaco 2015), moreover, the presence of the lateral outriggers was taken into account in the form of equivalent nodal restraints for the main log nodes (Fig. 4b).



(a) FE-model with outriggers

(b) FE-model with equivalent boundaries along the vertical edges

Fig. 4 Example of the typical FE-numerical model of a timber log-wall with single door opening (ABAQUS/Standard)

The mechanical interaction between logs composing the main tested walls was reproduced by means of suitable surface contact algorithms. Possible tangential sliding was allowed between the logs (*tangential behaviour*), with $\mu = 0.5$ being the static friction coefficient (Bedon and Fragiaco 2015). The detachment of logs in the direction perpendicular to the contact surfaces was also taken into account (*normal behaviour*), so that the influence of partial uplift and overturning of logs on the overall bending deformations of the examined log-walls could be investigated. Due to the presence of geometrical global curvatures and/or load eccentricities, this modelling feature proved to be a key parameter for the buckling behaviour of the log-walls loaded in compression.

Concerning the mechanical characterization of timber, C24 spruce was first described as an equivalent elasto-plastic, isotropic material having density $\rho= 420\text{kg/m}^3$, nominal average MOE perpendicular to the grain $E= 370\text{MPa}$, average shear modulus $G= 500\text{MPa}$ and Poisson's ratio calculated in accordance with Eq.(1). The occurrence of possible compressive damage and local failure mechanisms in the timber logs (e.g. localized crushing mechanisms along protrusions and grooves of main logs) was taken into account in the form of an average compressive strength $f_{c,90,m}= 3.57\text{MPa}$ of timber in the direction perpendicular to the grain.

Throughout the full parametric investigations, linear bifurcation analyses (LBA) were first carried out on each FE model, so that the fundamental buckling shape could be separately collected for all the log-wall configurations. The same FE models were then analysed under linearly increasing in-plane compressive loads N , by means of incremental nonlinear (INL) static simulations able to describe the full structural response of the examined log-walls up to collapse. The FE investigations were carried out to log-walls with in-plane rigid inter-storey floor (RF), as well as log-walls with fully flexible inter-storey floors (FF). In both cases, additional boundary restraints along the top log of each wall were properly implemented or removed, respectively (e.g. Fig. 4a).

4.2. Parametric study

Throughout the parametric FE-investigations, log-walls characterized by specific geometrical properties were assembled as described in Section 4.1, by varying the:

- a) total length L , with $H= 2.9\text{m}$ the reference nominal height for a single-storey building. A total log-wall length ranging from 3m to 6m with incremental steps of 0.5m was considered for each log wall configuration;
- b) nominal width b of each timber log, with $h= 16\text{cm}$ and 19cm respectively. Based on the cross-sections of timber log walls currently available on the market (www.rubnerhaus.com, www.perr-blockhaus.de, www.rusticasa.pt, www.lincolnlogs.com, www.polarlifehaus.com, www.loghomescotland.co.uk, www.satterwhite-log-homes.com, www.eurowood.co.nz), the total width of each log was varied from 8cm to 24cm, with an incremental step of 2cm, for each one of the examined log wall configurations;
- c) number and position of openings: no openings, single door or double door and/or window openings were taken into account;
- d) metal stiffeners for the openings (see Fig. 3b): for a given log-wall with door/window openings, INL simulations were carried out both with and without metal stiffeners along their vertical edges;
- e) restraint on the top log of the wall: either an in-plane fully rigid (RF) or fully flexible (FF) inter-storey floor was considered;

f) initial geometrical curvatures (with $u_{0,max}= H/400$ or $H/300$ the maximum amplitude) and/or load eccentricities e_{load} (with $b/6 \leq e_{load} \leq b/3$, in the current study).

In total, more than 900 log-wall configurations, obtained as a combination of the variables (a) to (f), were analysed through the parametric INL analyses. In the case of log-walls with single or double door/window openings, careful consideration was given to walls with reduced thickness b , as associated to high slenderness ratios and thus of primary interest for the purpose of the current FE study. Additional details on the examined configurations can be found in the tables of the Online Resource 1.

5. Discussion of FE results

The main results of this extended numerical investigation were properly assessed and compared, so that the structural effects of the main input parameters could be separately identified for a wide set of configurations of technical interest.

5.1. Initial curvature

Log-walls of different geometrical properties were first analysed considering an initial global curvature with various maximum amplitudes $u_{0,max}$, defined as the scaled LBA fundamental configuration for each geometry. As also shown in (Beton and Fragiaco 2015), the presence of initial geometrical imperfections typically result – depending on their maximum amplitude – in moderate decrease of the initial elastic stiffness for the examined log-walls. This effect typically leads to a premature overturning and detachment of few top logs only, with a progressive decrease of the global log-wall compressive resistance with respect to its corresponding Euler's critical load (e.g. Eqs.(1) and (2)).

Additional INL calculations with respect to those presented in (Beton and Fragiaco 2015) were carried out on preliminary deformed configurations, and the ultimate compressive load $(N_{max})_{INL}$ attained by each log-wall was separately collected. The results are presented in Figures 5 to 7.

Figure 5, for example, displays some of the non-dimensional curves obtained for log-walls characterized by various geometrical properties. Fig.5a presents the load N vs. $(u_{max} - u_{0,max})/H$ curves for log-walls without openings (RF configuration, $u_{0,max}= H/400$) characterized by fixed overall dimension ($L= 6\text{m}$ and $H= 2.9\text{m}$) and variable thickness of logs ($8 \leq b \leq 24\text{cm}$, with $h= 19\text{cm}$). As expected, for a given log-wall configuration, the corresponding buckling resistance and out-of-plane stiffness reduce as the thickness b decreases. However, in order to implement a practical analytical method of general applicability to mainly compressed timber log-walls, a multitude of aspects related to both geometrical features and mechanical effects should be taken into account.

Fig. 5b shows the variation of the predicted ultimate loads $(N_{max})_{INL}$ for several series of log-walls, namely characterized by $L=3\text{m}$ or $L=6\text{m}$ respectively, with the RF or FF restraint configurations and $8 \leq b \leq 24\text{cm}$ ($h= 19\text{cm}$). The

comparison between the collected FE data is carried out by taking into account the normalized slenderness ratio of each log-wall:

$$(\lambda_{crit,c})^* = \lambda_{crit,c} = \sqrt{\frac{f_{c,90,m} \cdot bL}{N_{cr,0}^{(E)}}} = \frac{\lambda}{\pi} \sqrt{\frac{f_{c,90,m}}{E_{\perp}}} \quad (10)$$

where $f_{c,90,m}$ denotes the mean compressive resistance of C24 spruce in the direction perpendicular to the grain, and $N_{cr,0}^{(E)}$ is separately calculated for each log-wall configuration (Eq.(1)).

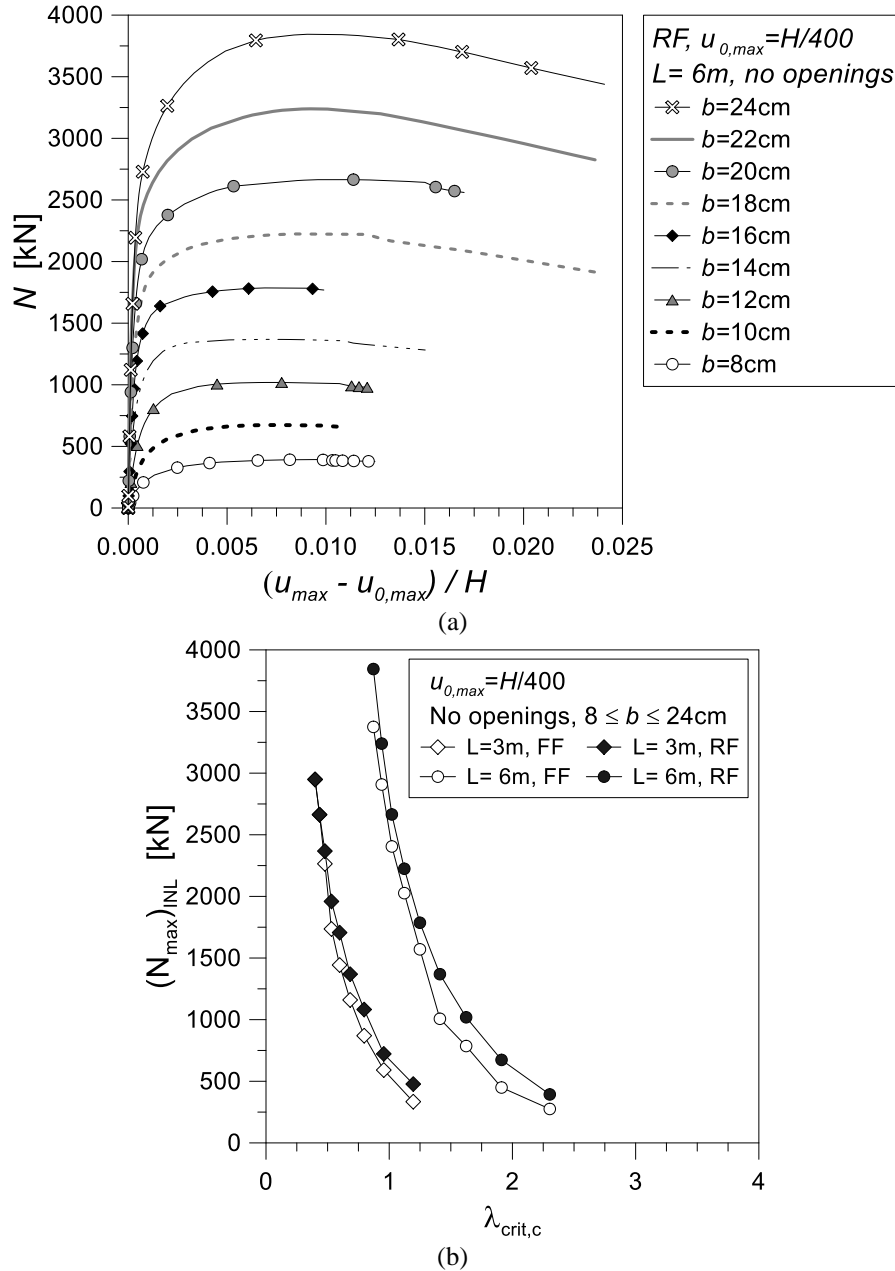


Fig.5 Comparative FE analysis results for in-plane compressed log-walls with initial geometrical curvature $u_{0,max} = H/400$. (a) Effect of thickness b variations, for a given log-wall geometry (RF configuration) and (b) effect of size variations (L , b) and restraint configurations (RF, FF) on the predicted buckling resistance $(N_{max})_{INL}$ values (ABAQUS/Standard).

As expected, for a given $L \times H$ geometrical configuration, the corresponding slenderness ratio (Eq.(10)) decreases as the thickness b increases. Accordingly, the ultimate buckling resistance $(N_{max})_{INL}$ increases, being the ultimate in-plane compressive behaviour of thick log-walls typically associated to pure local crushing mechanisms rather than buckling phenomena with large out-of-plane deformations. For the same reason, the presence of in-plane fully flexible inter-storey floors (FF) can be clearly recognized from the corresponding RF data for log-walls with high slenderness ratios. Based on the clear dependency of the collected FE data upon the geometrical features of each log-wall, as well as upon the value of the assigned initial imperfections, a further attempt to establish a general correlation between the so obtained FE ultimate resistance estimations was carried out by introducing a numerically predicted buckling coefficient:

$$(k_c)^* = k_c = \frac{(N_{max})_{INL}}{N_{res}} = \frac{(N_{max})_{INL}}{f_{c,90,m} \cdot b \cdot L} \quad (11)$$

Some relevant comparisons derived from the collected FE parametric results are displayed in dimensionless format in Figs. 6 and 7, for log-walls with RF or FF restraints respectively and two different imperfection amplitudes ($u_{0,max} = H/400$ and $H/300$).

The so derived FE data are also compared with additional analytical approximating curves, calculated in accordance with Eq.(8) and obtained by means of an appropriate numerical calibration of the β_c coefficient in Eq.(9), with $\beta_0 = 0.3$. This calibration was carried out based on the collected normalized FE data, so that the resulting curve given by Eq.(8) could be representative of the ultimate buckling resistance for most of the tested configurations.

In Fig. 6a, FE result are separately collected for log-walls without openings or single/double openings, respectively. As shown, the presence of door and window openings typically results in a marked increase of the normalized slenderness ratio (Eq.(10)) and decrease of the overall buckling resistance (Eq.(11)), compared to log-walls without openings. However, a sufficiently regular behaviour was found for all the investigated geometrical configurations, hence suggesting the conservative assumption of the proposed analytical curves for log-walls of different geometrical properties.

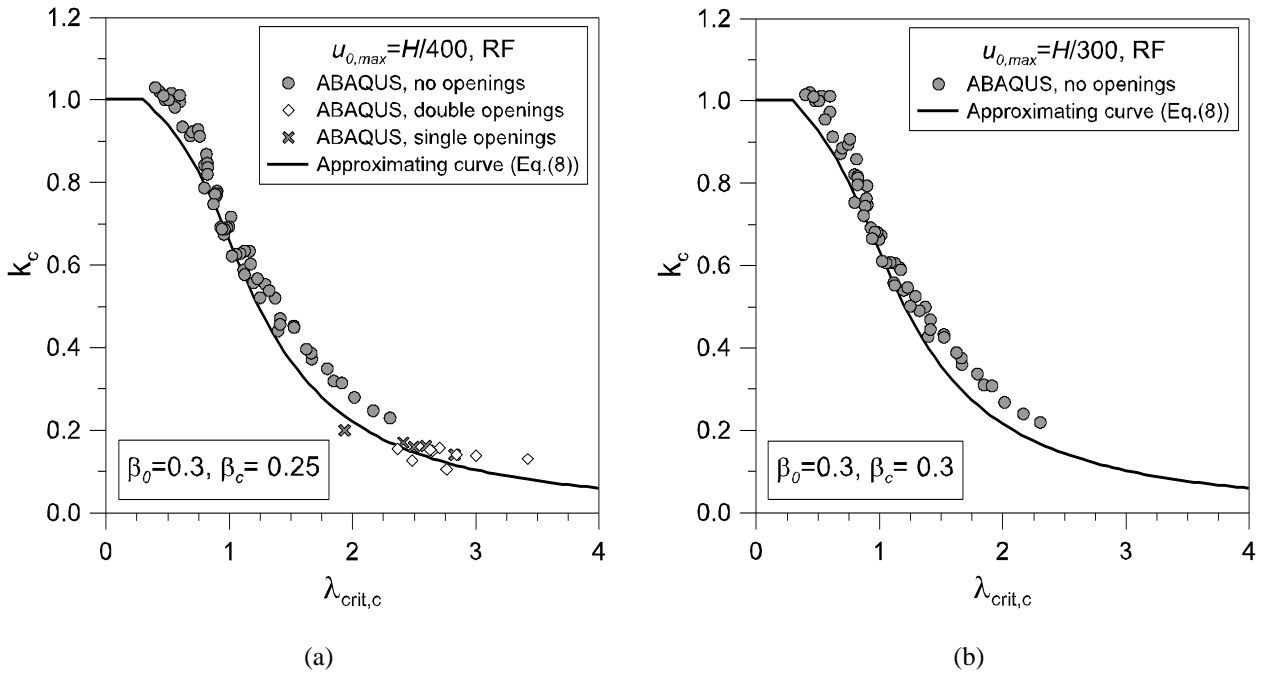


Fig. 6 Effect of initial curvatures $u_{0,max}$ on the buckling response of timber log-walls under in-plane compression (ABAQUS/Standard). Assumption of in-plane rigid inter-storey floor (RF)

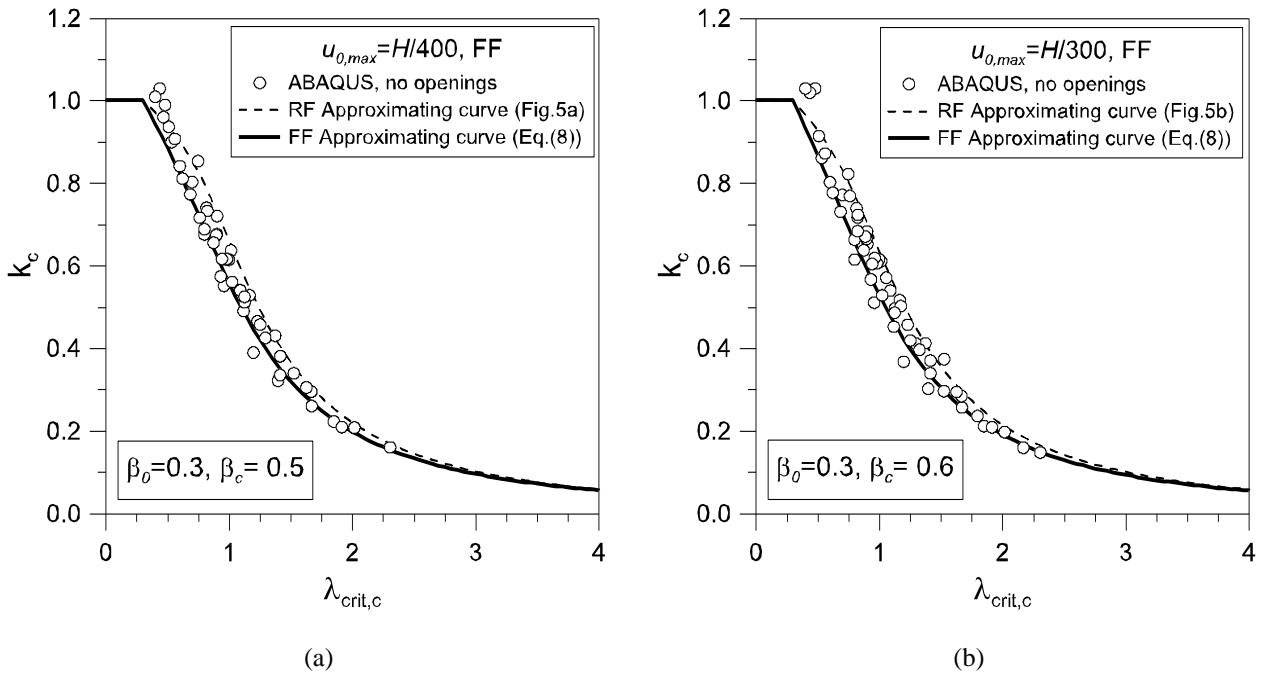


Fig. 7 Effect of initial curvatures $u_{0,max}$ on the buckling response of timber log-walls under in-plane compression (ABAQUS/Standard). Assumption of fully flexible inter-storey floor (FF)

Concerning the top lateral restraint offered by possible in-plane rigid inter-storey floors (Fig.7), as expected, a significant decrease of the predicted compressive ultimate loads was caused by the removal of these top boundaries. In

the FF configuration, the log-walls typically showed an average $\approx 30\%$ decrease in buckling resistance, compared to RF configurations, hence requiring the calibration of specific imperfection coefficients β_c (0.5 and 0.6 respectively for the configurations proposed in Fig.7) and careful consideration for the implementation of design recommendations. From a practical point of view, the main advantage of Eqs.(10) and (11) is represented by their general applicability to a given structural typology, once the key input imperfection factors are properly calibrated.

5.2. Load eccentricities

All the tested log-walls (see the Online Resource 1) also showed a high sensitivity to possible load eccentricities e_{load} (with $b/6 \leq e_{load} \leq b/3$ in the current parametric study), due to the intrinsic design concept of timber log-wall structural systems.

The application of compressive loads N with a small eccentricity e_{load} , typically resulted in the premature, partial overturning of the top logs, with progressive detachment of the resisting surfaces in contact and hence an abrupt decrease of the overall compressive load-carrying capacity. Comparative examples are displayed in Fig. 8 for a selected geometrical configuration (log-wall without openings, with $b=12\text{cm}$ and $h=19\text{cm}$, $H=2.95\text{m}$, $L=4\text{m}$, RF configuration), by varying the assigned load eccentricity e_{load} .

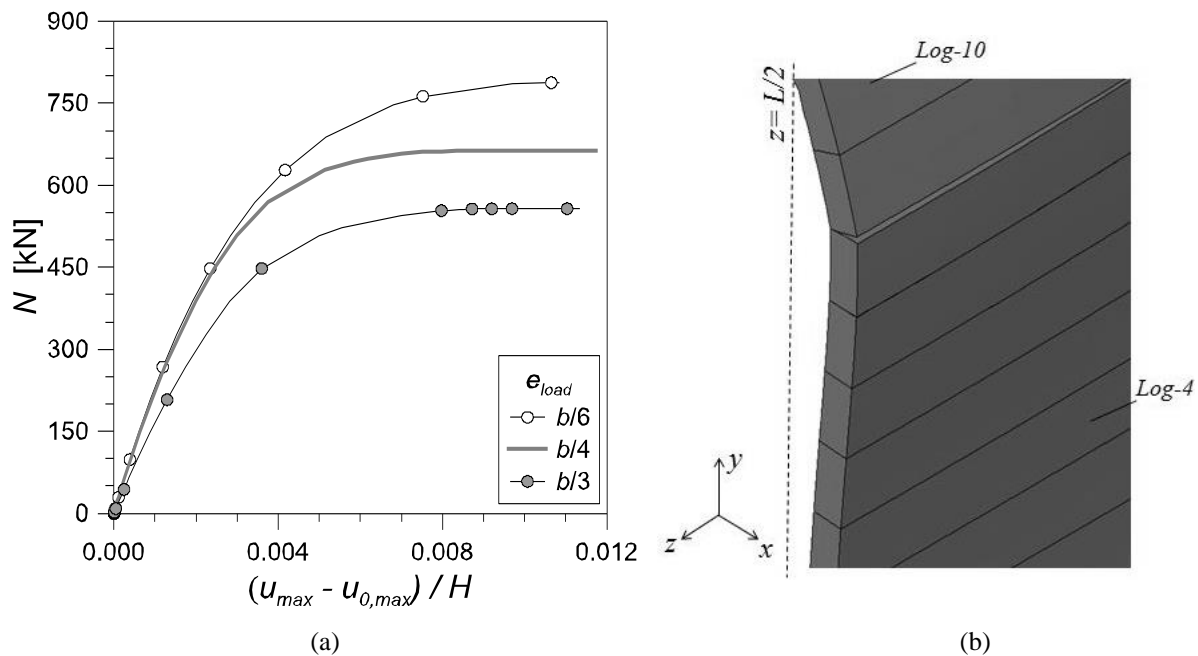


Fig. 8 Effect of load eccentricities e_{load} on the buckling response of timber log-walls under in-plane compression (ABAQUS/Standard). Assumption of in-plane rigid inter-storey floor (RF). (a): compressive load vs. non-dimensional out-of-plane deformations; (b): detail of the qualitative deformed shape (ABAQUS/Standard)

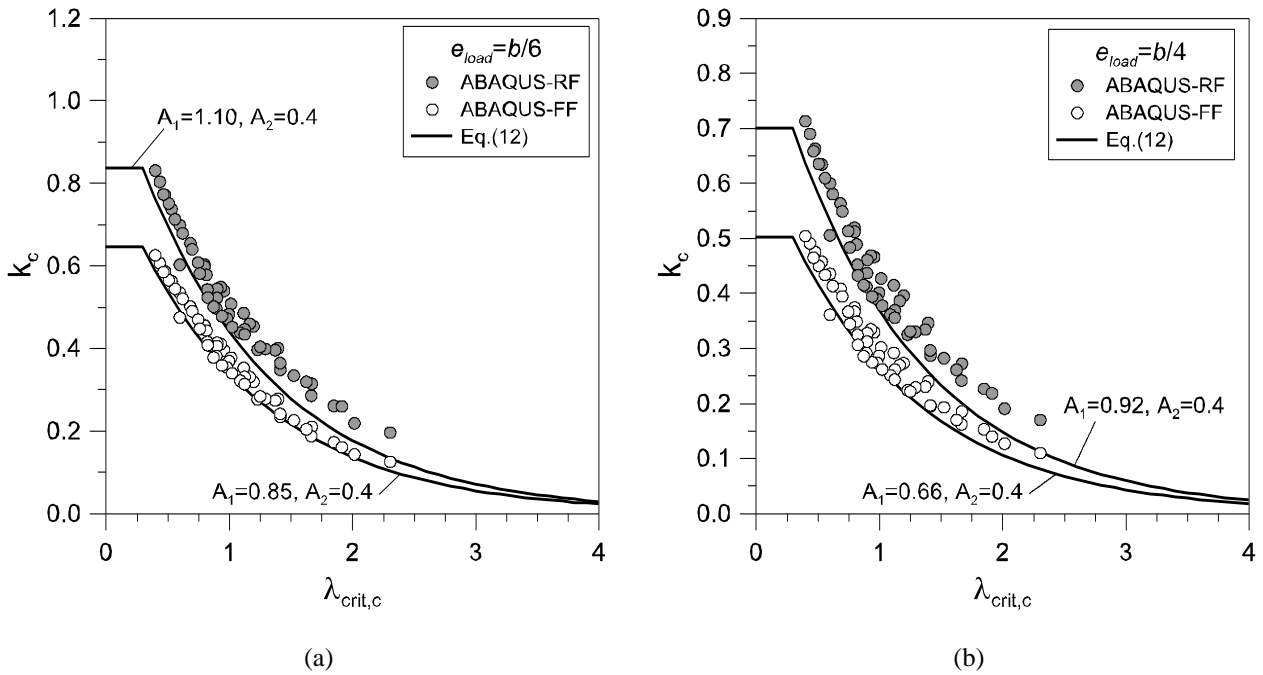
Additional comparative FE parametric results are also collected in dimensionless format (e.g. see Eqs.(10) and (11)) in Fig. 9. In general, for all the examined geometrical configurations, an almost exponential relationship can be found

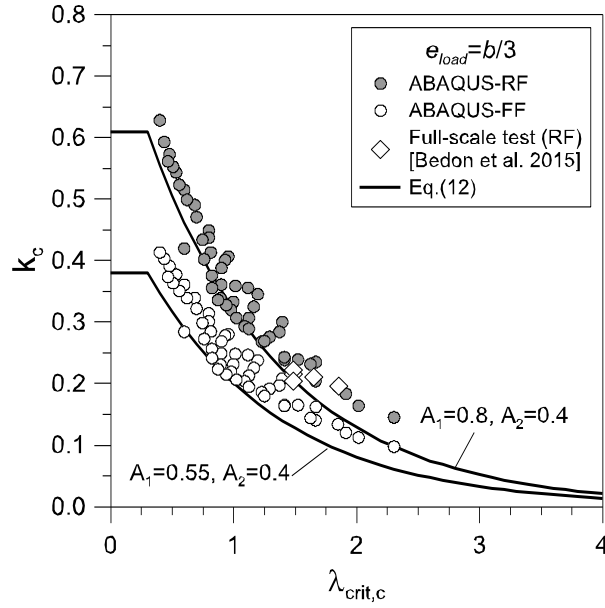
between the log-wall slenderness ratio and the corresponding buckling reduction coefficient k_c , for a given load eccentricity, given by:

$$k_c = A_1 A_2^{\lambda_{crit,c}}, \quad (12)$$

In Eq.(12), the constants A_1 and A_2 depend on the sensitivity of each log-wall configuration and top restraint condition (e.g. RF or FF restraint) to the assigned load eccentricity e_{load} , and can approximately be estimated as suggested in Fig. 9 (with $0.3 \leq \lambda_{crit,c} \leq 4$). The parametric FE study also highlighted that an almost constant value of 0.4 can be used for A_2 , independently of the assigned eccentricity amplitude.

In the same Fig. 9, it can be seen that the absence of the top lateral restraints (e.g. FF configuration) markedly affects the actual compressive resistance of the examined log-walls, and in the current study typically resulted in overestimations up to $\approx 30\%$ of the actual compressive resistance of the same log-walls with in-plane rigid inter-storey floors (e.g. RF restraint). In Fig.9c, the experimental estimations obtained from full-scale (RF) buckling experiments discussed in (Bedon et al. 2015) are also shown, as a further assessment of the calibrated approximating curves.





(c)

Fig. 9 Effect of load eccentricities e_{load} on the compressive buckling resistance of timber log-walls. Assumption of in-plane rigid (RF) or fully flexible (FF) inter-storey floor. FE numerical data (ABAQUS/Standard) and corresponding conservative approximating curves (Eq.(12))

5.3. Combined initial curvature and load eccentricity

The application of combined initial geometrical curvature $u_{0,max}$ and load eccentricity e_{load} was also investigated, being this case of relevance for the development of general design recommendations.

This last series of parametric analyses typically resulted – compared to Sections 5.1 and 5.2 – in a further amplification of the destabilizing effects deriving from curvatures or load eccentricities only, hence leading to a further decrease of the log-wall initial stiffness (see for example Fig. 10a, where the results of a log-wall without openings are proposed, with $b=12\text{cm}$ and $h=16\text{cm}$, $H=2.95\text{m}$, $L=4\text{m}$, RF configuration) and a premature detachment of the top logs, with consequently a reduction of the actual load-carrying capacity for the studied log-walls. For all the examined geometrical configurations, the simultaneous application of initial global curvatures of maximum amplitude $u_{0,max}=H/400$ and load eccentricities e_{load} ($b/6 \leq e_{load} \leq b/3$) generally led to an average $\approx 5\%$ decrease of the buckling resistances calculated, for the same set of log-wall configurations, in presence of eccentricities e_{load} only. This can be noticed from Fig. 10b, where the results of INL parametric analyses (Eqs.(10) and (11)) are displayed in dimensionless format together with the corresponding analytical conservative approximations (Eq.(12)) for log-walls with fully rigid top lateral restraint (RF).

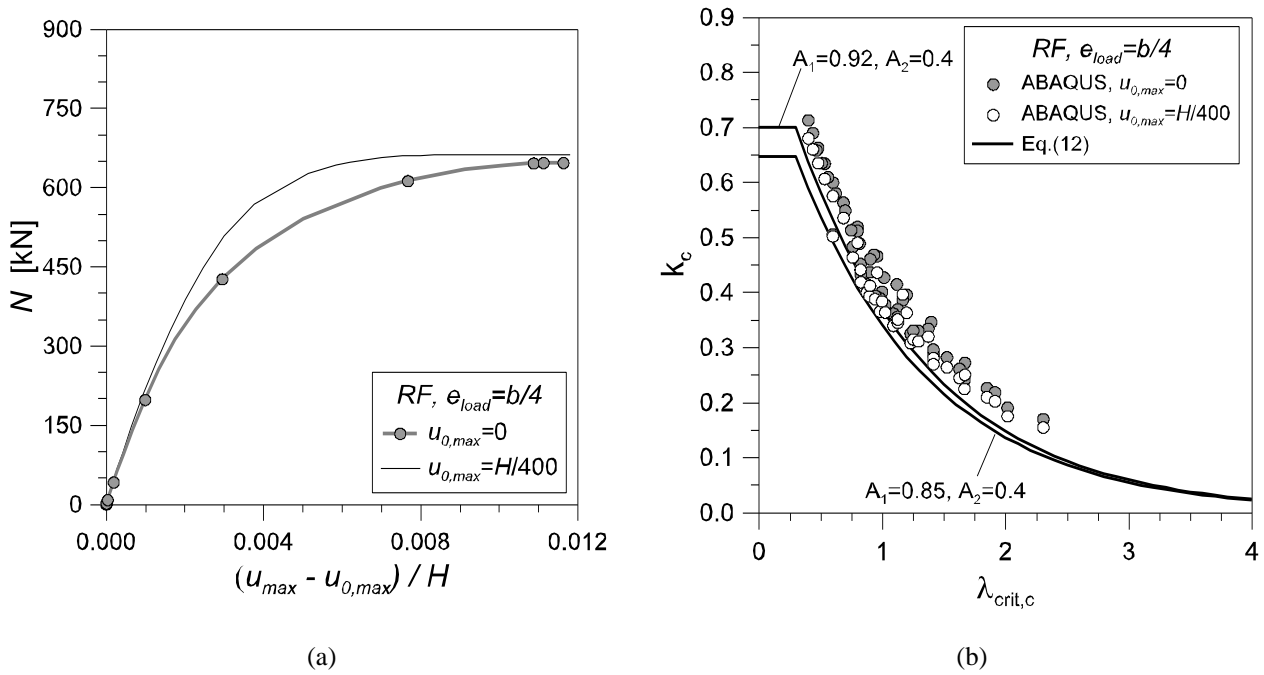


Fig. 10 Effect of combined initial curvature and load eccentricity e_{load} on the compressive buckling resistance of timber log-walls. Assumption of in-plane rigid inter-storey floor (RF). (a): compressive load vs. non-dimensional out-of-plane deformations; (b): FE numerical data (ABAQUS/Standard) and corresponding conservative approximating curves (Eq.(12))

5.4. Log-walls under combined in-plane compression and out-of-plane pressures

Final assessment of the expected structural response for the examined log-walls was carried out by taking into account the combination of in-plane compressive loads N and additional out-of-plane pressures q_h , uniformly distributed on the log-wall surface (e.g. wind pressures acting simultaneously to compressive loads N), see Fig.11.

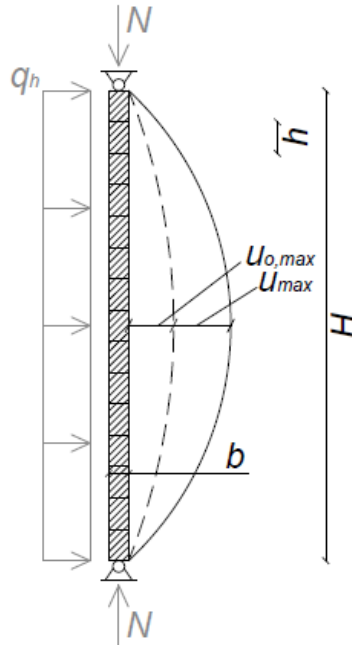


Fig 11 Reference model for the buckling analysis of log-walls under in-plane compressive loads N , with simultaneous initial curvatures $u_{0,max}$ and out-of-plane pressures q_h (vertical wall cross-section, with the assumption of RF configuration and no openings)

In order to numerically investigate the structural performance of log-walls subjected to combined loads, the FE method described in Section 4.1 was used. Once defined the geometry for a given log-wall, a preliminary LBA simulation was carried out for in-plane compressive loads N only. The so obtained fundamental buckling shape was then scaled to the desired maximum amplitude $u_{0,max}$ and assumed as a reference geometrical configuration for the corresponding INL analysis. Through the INL simulations, unlike Section 4.1, each log wall was ramp loaded by increasing the in-plane compressive load N and considering a uniformly distributed, constant pressure q_h . The ultimate buckling resistance $(N_{max})_{INL}$ of each log-wall was then separately collected as in Section 5.

Compared to the buckling performance of in-plane compressed walls only, and to the related analytical methods derived from the Eurocode 5 for timber members in compression, in this latter loading condition a different approach was considered for the implementation of practical design recommendations.

With reference to Fig.11, the expected ultimate compressive resistance N_{max} of the examined log-wall can be approximately calculated by taking into account the effects of the applied out-of-plane pressures q_h , together with possible geometrical imperfections, by introducing the concept of equivalent curvature due to q_h .

In order to assess the validity of this approach, further FE simulations were carried out on some of the log-wall configurations without openings listed in the Online Resource 1. Some of the so derived comparative examples are collected in Fig. 12a, for a given log-wall with $b=8\text{cm}$ and $h=19\text{cm}$, $H=2.95\text{m}$, $L=3\text{m}$, (RF condition), where an initial curvature of maximum amplitude $u_{0,max}=H/400$ was considered. Several values of the assigned constant pressure

q_h (100, 500, 1000 and 1500 N/m² respectively) were considered while linearly increasing the in-plane compressive loads N up to failure.

As shown in Fig.12a, the parametric simulations highlighted that an increase in the assigned pressure q_h leads to a modification of the reference geometrical configuration for the same log-wall, hence resulting in a gradually increasing $(u_{max} - u_{0,max})/H$ initial curvature on which the in-plane compressive loads N are applied (e.g. imperfection amplitudes for $N=0$).

A nonlinear correlation was found, however, between the assigned out-of-plane pressures q_h and the corresponding initial curvature or ultimate buckling resistance for the tested log-walls. This effect can be clearly seen from Fig.12b and can be rationally justified by the design concept of *Blockhaus* structural systems, that is by the intrinsic discontinuity of the log-walls due to the presence of stacked and mainly disjointed timber logs. For this reason, the combination of initial curvatures $u_{0,max}$ with out-of-plane pressures q_h and in-plane compressive loads N typically leads to further local destabilizing effects that should be properly taken into account in design. A practical example is shown in Fig.12c, for the same log-wall geometry, in the form of a contour plot of out-of-plane displacements ($N=420$ kN, $q_h=1500$ N/m²). The partial overturning at the bottom of the log-wall can be clearly distinguished.

A final attempt to derive a general analytical method for the examined loading configuration, based on the observed numerical results, was thus carried out by comparing the so collected ultimate FE data $(N_{max})_{INL}$ in non-dimensional form by means of Eq.(11), see Fig.12d.

The corresponding normalized analytical curve of Fig. 12d is calculated as:

$$(k_c)_{an} = \chi_{imp} \frac{N_{cr,o}^{(E)}}{N_{res}} = \left(1 - \frac{e + e_{q_h}}{b} \right) \frac{N_{cr,o}^{(E)}}{f_{c,90,m} \cdot bL} \quad (13)$$

with $e = u_{0,max}$ and

$$e_q = \frac{M_{q,max}}{(N_{max})_{q_h=0}} \quad (14)$$

signifying the imperfection representative of the assigned out-of-plane pressures q_h .

In Eq.(14), the maximum bending moment due to q_h can be approximately calculated by assuming the log-wall as simply supported at the top and bottom edges (see Fig.11), that is:

$$M_{q,max} = \frac{(q_h L) \cdot H^2}{8} \quad (15)$$

In Eq.(14), moreover,

$$(N_{\max})_{q_h=0} = \left(1 - \frac{e}{b}\right) \frac{N_{cr,0}^{(E)}}{f_{c,90,m} \cdot bL} \quad (16)$$

represents the ultimate compressive resistance of the same log-wall without out-of-plane pressures (e.g. $q_h = 0$, with $e = u_{0,max}$).

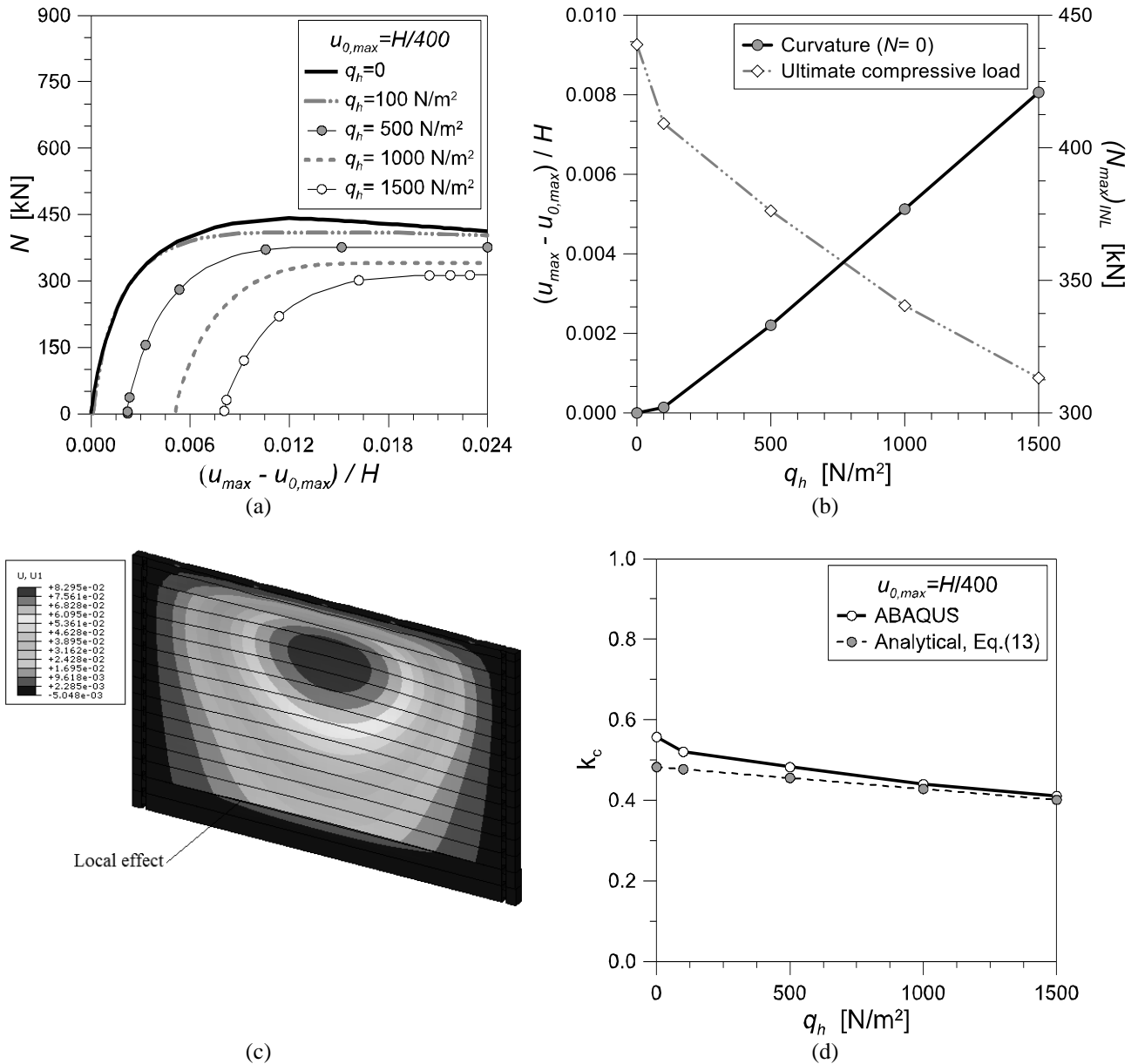


Fig. 12 Effect of out-of-plane pressures q_h acting simultaneously to in-plane compressive loads N ($H=2.95$ m, $L=3$ m, $b=8$ cm; RF configuration), with $u_{0,max} = H/400$: (a) dimensionless compressive load – out-of-plane deflection curves. (b)

Qualitative effect of out-of-plane pressures q_h and initial curvatures $u_{0,max}$ on the buckling response of an in-plane compressed timber log-wall with a (c) typical deformed configuration due to N - q_h loads (displacements in meters, $N=420$ kN, $q_h=1500$ N/m²). (d) buckling coefficient k_c depending on out-of-plane pressure q_h

As shown in Fig. 12b, despite the simplified assumptions of the adopted approach, a rather close agreement was found between the collected FE-INL data and the corresponding analytical calculations, hence suggesting the validity of the proposed simplified analytical approach. It is thus concluded that the same analytical procedure could be also conservatively extended to log-walls with openings as well as under the FF restraint configuration.

6. Proposal of a standardized buckling design method for timber log-walls

In order to implement a standardized buckling design method of practical use, further INL parametric investigations were finally carried out on the same log-wall configurations described in Section 4.2 and in the Online Resource 1, by replacing in all the FE models the mean mechanical properties of C24 spruce with the corresponding design values:

$$E_{\perp,d} = \frac{E_{\perp}}{\gamma_M}, \quad G_d = \frac{G}{\gamma_M} \quad \text{and} \quad f_{c,90,d} = \frac{k_{\text{mod}} f_{c,90,k}}{\gamma_M} \quad (17a) \quad (17b) \quad (17c)$$

with $\gamma_M = 1.3$ the partial safety factor of wood (EN 1995-1-1-2005), $f_{c,90,k} = 2.5\text{MPa}$ the characteristic value of the compressive strength perpendicular to the grain (EN 338:2009) and $k_{\text{mod}} = 0.7$ the partial modification factor for moisture and load duration influence (service class 1 and 2, and imposed load of long-term duration according to (EN 1995-1-1-2005)). A practical example is proposed in Fig.13a, where the INL results obtained for three log-walls ($L \times H$ the overall dimensions and b the log width, with $u_{0,\text{max}} = H/400$) by taking into account the mean ('ABAQUS, mean properties') or design ('ABAQUS, design properties', e.g. Eqs.(17a)-(17c)) mechanical properties of timber are shown. In both the cases, the INL data are normalized by means of Eqs.(10) and (11), with the corresponding mean or design elastic properties for timber. The critical load $N_{cr,0}^{(E)}$ in Eq.(10) is calculated by means of Eq.(1), with mean or design elastic moduli respectively. The labels 'A', 'B' and 'C', finally, denote respectively three different log-wall geometries selected from the full list of possible combinations of the input variables provided in Section 4.2 (see also in the Online Resource 1).

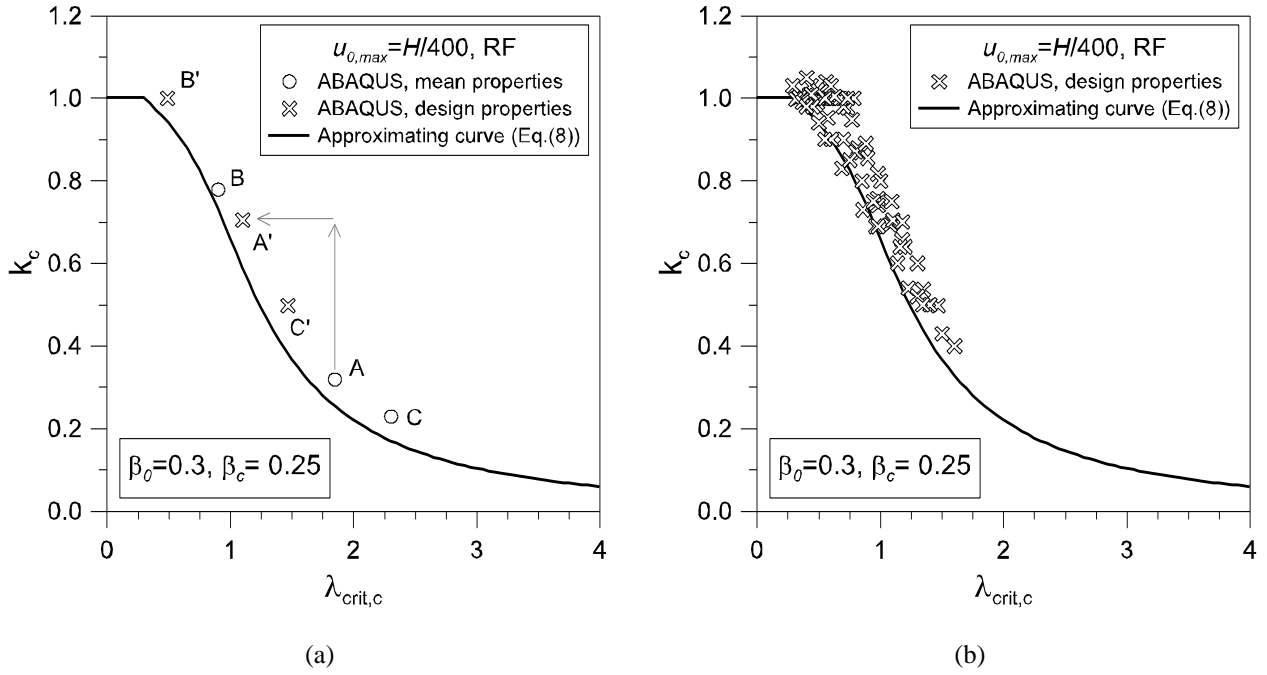


Fig. 13 Validation of the buckling design approach for log-walls with initial geometrical curvatures. (a) Qualitative effect of using design mechanical properties for timber; (b) FE parametric study with design properties of timber

As shown, the main effect from the use of the design elastic moduli and compressive strength for timber is a shift of the predicted INL data presented in Section 5. Due to the appropriate calibration of the β_0 and β_c imperfection factors for the conservative approximating curve (Eq.(8)), however, since these values are representative of the effects from possible initial curvatures $u_{0,max}$, the same values 0.3 and 0.25 proposed in Section 5.1 can be used for design purposes . Similarly, when load eccentricities e_{load} or combined curvatures / eccentricities are present, the constants A_1 and A_2 derived in Section 5.2 and 5.3 for the approximating curve (Eq.(12)) are still valid (see Figs. 13a and 13b).

In conclusion, in accordance with the existing Eurocode 5 approach for timber members in compression, the buckling design verification of log-walls subjected to in-plane compressive design loads N_{sd} can be expressed as:

$$N_{b,Rd} = k_c \cdot \left(N_{cr,0}^{(E)} \right)_d \geq N_{sd}, \quad (18)$$

with k_c and $\left(N_{cr,0}^{(E)} \right)_d = f(E_{\perp,d}, G_d)$ given in Table 1.

For intermediate values of initial imperfection $u_{0,max}$ and load eccentricity e_{load} , a linear interpolation between the values of $N_{b,Rd}$ obtained according to Table 1 can be used to estimate the corresponding load-carrying capacity of a given log-wall loaded in-plane.

The presence of a possible uniformly distributed out-of-plane pressure q_h acting simultaneously to the assigned in-plane compressive load N , in accordance with Section 5.4, can be also reasonably taken into account in the form of an equivalent additional eccentricity given by Eqs. (14) and (15).

Table 1 Conservative approximating curves of k_c , with the corresponding imperfection factors and design critical loads for timber log-walls under in-plane compression and subjected to initial curvatures and/or load eccentricities

		No openings / Single opening / Double openings		$(N_{cr,0}^{(E)})_d$				
		Imperfection / Eccentricity	Approximating curve	In-plane rigid floor (RF)	Fully flexible floor (FF)	No openings	Single opening	Double openings
Curvature only	$u_{0,max} = H/400$	Eq.(8), with $\beta_0 = 0.3$	$\beta_c = 0.25$	$\beta_c = 0.3$	Eq.(1)	Eq.(1) with $L = L_{ef}$	Eq.(2)	
	$u_{0,max} = H/300$		$\beta_c = 0.5$	$\beta_c = 0.6$				
Eccentricity only	$e_{load} = b/6$	Eq.(12), with $A_2 = 0.4$	$A_1 = 1.10$	$A_1 = 0.85$				
	$e_{load} = b/4$		$A_1 = 0.92$	$A_1 = 0.66$				
	$e_{load} = b/3$		$A_1 = 0.80$	$A_1 = 0.55$				
	$u_{0,max} = H/400$ + $e_{load} = b/4$		$A_1 = 0.85$	$A_1 = 0.60$				

7. Conclusions

This paper analyses the buckling response of timber log-walls under in-plane compression via an extended FE parametric investigation validated towards past analytical and experimental data. Careful consideration was given both to the influence of several geometrical aspects (e.g. log-wall dimensions, timber log cross-section, presence and position of door / window openings) and to further influencing parameters, like initial curvatures and / or load eccentricities of different amplitude. The effects of additional out-of-plane curvatures acting simultaneously to the in-plane compressive loads were also assessed.

Conservative approximating curves were then properly calibrated, based on the collected FE parametric results and on analytical methods derived from the Eurocode 5 for timber structures, in order to provide normalized design curves for the buckling verification of the examined log-walls. Despite the high susceptibility of ‘*Blockhaus*’ systems to buckling phenomena, due to the reduced mechanical properties of timber perpendicular to the grain as well as to the specific design concept of log-wall structural systems, the current Eurocode 5 for timber structures does not provide formulations and recommendations for the prediction of the critical load.

A standardized buckling design method, conceptually similar to that used for the design of timber columns, was thus properly modified and proposed.

The implicit advantage of the current proposal is given by the accurate FE calibration and validation of existing buckling design procedures to the studied structural system. All the important variables affecting the buckling load-carrying capacity of log-walls, like geometrical properties, presence or not of openings, restraint offered by the floor, initial curvature, load eccentricity, and out-of-plane pressure such as that due to wind can in fact be properly taken into account by means of equivalent imperfection coefficients and analytical expressions of practical use. The so calibrated normalized curves were found to provide a simple and conservative solution, compared to FE data as well as full-scale experimental test results. It is thus expected that the proposed recommendations could be further extended and implemented in the ongoing revision of the current standards for timber structures.

Acknowledgements

DPC-ReLUIIS is gratefully acknowledged for partially funding the research activity within the framework of the "PR4-Timber structures" project.

References

- Baláz I (2005): Lateral torsional buckling of timber beams, *Wood Research*, 50(1): 52-58
- Bedon, C, Fragiacom, M (2015): Numerical and analytical assessment of the buckling behaviour of Blockhaus log-walls under in-plane compression. *Engineering Structures*, 82: 134-150
- Bedon, C, Rinaldin, G, Izzi, M, Fragiacom, M, Amadio, C (2015): Assessment of the structural stability of Blockhaus timber log-walls under in-plane compression via full-scale experiments. *Construction and Building Materials*, 78: 474-490
- Bouras F, Chaplain M, Nafa Z (2010): Experimental and modeling buckling of wood-based columns under repeated loading, *Proceedings of the 14th International Conference on Experimental Mechanics*, Poitiers, France, 4-9 July 2010, code 110074
- Bouras F, Chaplain M, Nafa Z, Breyse D, Tran H (2012). Experimental behavior of wood columns under extreme loading: cyclic buckling. *Proceedings of the World Conference on Timber Engineering WCTE 2012*, Volume 5, pp.545-550
- Eilering S, Beißner E (2011): On the stability of circular curved beams of glue-laminated timber [Zur Stabilität von BSH-Kreisbogenbindern], *Bauingenieur*, 86(2): 76-83
- EN 338: 2009. Structural timber-strength classes. European Committee for Standardization (CEN), Brussels, Belgium
- EN 1993-1-1: 2005 - Eurocode 3 – Design of steel structures – Part 1-1: general rules and rules for buildings. European Committee for Standardization (CEN), Brussels, Belgium
- EN 1995-1-1-2005 - Eurocode 5 – Design of timber structures - Part 1-1: General and rules for buildings. European Committee for Standardization (CEN), Brussels, Belgium
- EN 1996-1-1:2005 - Eurocode 6 - Design of masonry structures - Part 1-1: General rules for reinforced and unreinforced masonry structures, European Committee for Standardization (CEN), Brussels, Belgium
- EuroWood Construction (NZ), www.eurowood.co.nz
- Haller P, Hartig J, Wehsener K (2014): Application of moulded wooden tubes as structural elements, *Proceedings of the World Conference on Timber Engineering WCTE2014*, Quebec City, Canada, 10-14 August 2014; Code 110957
- Heimeshoff, B, Kneidl, R (1992a): Zur Abtragung vertikaler Lasten in Blockwänden – Experimentelle Untersuchungen. *Holz als Roh – und Werkstoff*, 50: 173-180. Springer-Verlag
- Heimeshoff, B, Kneidl, R (1992b): Bemessungsverfahren zur Abtragung vertikaler Lasten in Blockwänden. *Holz als Roh – und Werkstoff*, 50: 441-448. Springer-Verlag
- Hofmann R, Kuhlmann U (2014): Simplified Design of Glued Laminated Timber Girders for the Torsional Moment Caused by Stability Effects, *Materials and Joints in Timber Structures*, pp-823-830, ISBN 978-94-007-8710-8

- Kessel MH (2012): Imperfections of pitched timber trusses [Imperfektionen von satteldachförmigen fachwerkträgern aus holz], *Bauingenieur*, 87(1): 277-287
- Leicester RH (2009): Buckling strength of timber structures, *Australian Journal of Structural Engineering*, 9(3): 249-256
- LogHomeScotland (United Kingdom), www.loghomescotland.co.uk
- Malhotra SK (1989): Recent developments relating to design of solid and built-up timber compression members, *International Journal for Housing Science and its Applications*, 13(1): 35-44
- Namiki H, Nasu H (2014): Study on prevention for buckling of combined pillar with fiber materials or screws, *Proceedings of the World Conference on Timber Engineering WCTE2014*, Quebec City, Canada, 10-14 August 2014; Code 110957
- PERR Blockhäuser (Germany), www.perr-blockhaus.de
- Polar Life Haus® (Finland), www.polarlifehaus.com
- Rodman U, Saje M, Planinc I, Zupan D (2013): The lateral buckling of timber arches, *International Journal of Structural Stability and Dynamics*, 13(08), 16 pages, doi: 10.1142/S0219455413500405
- Rubner Haus AG Spa (Italy), www.rubnerhaus.com
- Rusticasa Construções Lda (Portugal), www.rusticasa.pt
- Satterwhite Log Homes (TX, USA), www.satterwhite-log-homes.com
- Simulia (2012). ABAQUS v.6.12 Computer Software, Dassault Systems, Providence, RI, USA
- Schnabl S, Turk G, Planinc I (2011): Buckling of timber columns exposed to fire, *Fire Safety Journal*, 46(7): 431-439
- Taheri F, Nagaraj M, Khosravi P (2009): Buckling response of glue-laminated columns reinforced with fiber-reinforced plastic sheets, *Composite Structures*, 88(3): 481-490
- The Original Lincoln Logs® (NY, USA), www.lincolnlogs.com
- Theiler M, Frangi A, Steiger R (2013): Strain-based calculation model for centrally and eccentrically loaded timber columns, *Engineering Structures*, 53(11): 1103-1116
- Zahn JJ (1973): Lateral stability of wood beam-and-deck systems, *ASCE J Struct Div*, Vol. 99, Issue ST7, pp. 1391-1408
- Xiao Q, Doudak G, Mohareb M (2014): Lateral torsional buckling of wood beams: FEA-modelling and sensitivity analysis, *Proceedings of the World Conference on Timber Engineering WCTE2014*, Quebec City, Canada, 10-14 August 2014; Code 110957